

Supporting Information

Sunlight-mediated Photocatalytic Uranium Extraction from Seawater: A Bioresistant Heterojunction for Highly Selective Uranium Sensing and Extraction with In-vivo Application†

Sanjay Yadav,*^{ac} Nishu Choudhary,^{ac} Vasavdutta Sonpal,^{bc} Bipin G. Vyas,^{ac} and Alok Ranjan Paital*^{ac}

E-mail: arpaital@csmcri.res.in; sychem00700@gmail.com.

Table of Content

Sr. No	Contents	Page No.
1	Materials & Methods	S2
2	Synthesis of Ionic liquid & Materials (CD@WFNS, CD@WFNS@Cl, WFNS@DAB-AO) (Fig. S1-2).	S3-6
3	Photophysical, Adsorption, Biosensing & Antibacterial studies	S6-9
4	The FeSEM EDX analysis & elemental mapping of the WFNS and CD@WFNS material (Fig. S3-4).	S9-10
5	The Pore size, PXRD & FTIR profiles (Fig. S5-6)	S10-11
6	The P-2p & N 1s core shell spectra of the CD@WFNS material, the O 1s & S-2p core shell spectra of the final material CD@WFNS@DAB-AO (Fig. S7-8).	S12
7	The UV-Vis & the excitation independent spectra of the final materials (Fig. S9-10).	S13
8	The pH dependent studies & selectivity profile with the anions (Fig. S11-12).	S14
9	The Fluorescence response, Linear range and stability studies (Fig. S13-14).	S15
10	The comparison of the fluorescence emission plot of the starting material CD@WFNS and final material CD@WFNS@DAB-AO and the Freundlich adsorption isotherms (Fig. S15-16).	S16
11	The adsorption capacity of WFNS & competitive extraction analysis ICP-MS (Table S1), the EDX analysis, the elemental mapping & the HR TEM analysis of the material post uranium adsorption (Fig. S17-20).	S17-19
12	The colour change pictures of the material before and after uranium adsorption Zeta Potential, % Removal plot, (Fig. S21-23) the adsorption kinetics parameters (Table S2),	S19-20
13	The regeneration studies with fluorescence tracking, the characterization of the original and the regenerated material & The core-shell O 1s & N 1s spectra of the uranium adsorbed material (Fig. S24-26)	S21-22
14	The fluorescence lifetime spectra & the EPR analysis results (Fig. S27-28).	S23
15	The Field test (natural seawater uranium extraction) (Fig. S29) and the comparison table (Table S3).	S24-29

Materials & Methods

Materials: All chemicals and reagents used in chemical processing and synthetic procedures were of analytical grade. Dry solvents were employed without additional purification steps. For the synthesis of materials, urea, triethylamine, TEOS, 1-decanol, Butanol, formaldehyde, Sodium citrate, phytic acid, hydroxylamine hydrochloride, 3-CPTES were purchased from Merk (Sigma-Aldrich), 2,2,6,6- Tetramethylpiperidine1-Oxyl Free Radical (TEMPO), 5,5-Dimethyl-1-pyrroline N-oxide (DMPO) as spin trapping agents & HEPES buffer were purchased from TCI Chemical Private Ltd & Merk (Sigma-Aldrich). 2,4-Diaminobenzonitrile was purchased from Zeta Scientific. Dry toluene, Milli-Q water, HCl, NaOH, methanol, chloroform, and chloride and nitrate salts of cations, potassium and sodium salts of anions were sourced from Suvidhinath Laboratories and Spectrochem Pvt. Ltd.

Instrumentation: Absorption and fluorescence emission spectra were recorded using a Shimadzu UV 3101PC spectrophotometer and an Edinburgh Instruments model Xe-900, with a 500 nm excitation source, in an aqueous dispersion medium. Perkin-Elmer GX spectrophotometer (USA) with KBr pellets was used for FTIR spectra measurements. Surface area measurements were conducted using a Micromeritics 3 FLEX instrument, with samples activated at 60 °C for 45 min before analysis. Scanning electron microscopy (SEM-Leo series 1420 VP) equipped with INCA and transmission electron microscopy (TEM) using a JEOL JEM 2100 microscope was employed for surface morphology analysis, both using Lacey carbon-coated grids. X-ray photoelectron spectroscopy (XPS) analysis was performed using a Thermo Fisher Nexsa spectrophotometer with monochromated Al K α radiation at 1486.6 eV energy. Metal ion concentration determination was carried out using an ICP-MS Thermo Fisher iCAP Qnova series instrument, with samples filtered using Thermo Fisher syringe filters (0.45 μ m). Powder X-ray diffraction profiles were recorded using a Rigaku MiniFlex-II (FD 41521) powder diffractometer from Japan, with a scan rate of 1° per min. EPR spectra were recorded on MiniScope MS-5000 bench top EPR/ESR Spectrometer consisting of Spectrometer mainframe. Fluorescence lifetime measurements were conducted using TSPC experiments on an Edinburgh Instruments OB 920 fluorescence spectrophotometer equipped with a pulse diode laser (Laser-EPLED-480 nm) as the excitation source.

Experimental section:

Synthesis of 1-methyl-3-octadecyl-1H-imidazol-3-ium bromide ionic liquid template

For the synthesis of 1-methyl-3-octadecyl-1H-imidazol-3-ium bromide ionic liquid, 2.5 mL (31.36 mmol) of methyl imidazole and 6 mL (17.56 mmol) of 1-bromo octadecane was refluxed in 150 mL ethanol at 78 °C for 48 h. After reaction times, the solvent was rotary evaporated, giving out a white powder. Further purification of the compound was conducted by recrystallization from ethyl acetate to afford 4.89 g of white, shiny powder, which was characterized by ^1H and ^{13}C NMR spectroscopy.

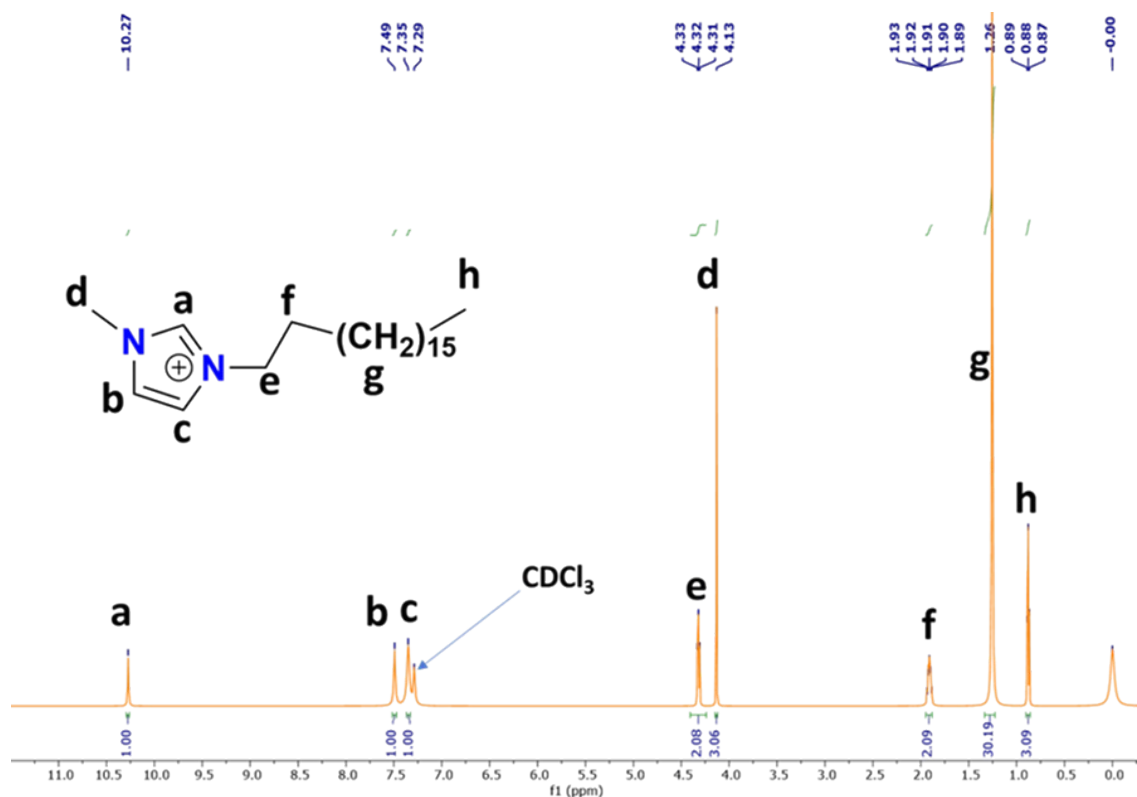


Fig. S1 ^1H NMR spectra of the synthesized ionic liquid.

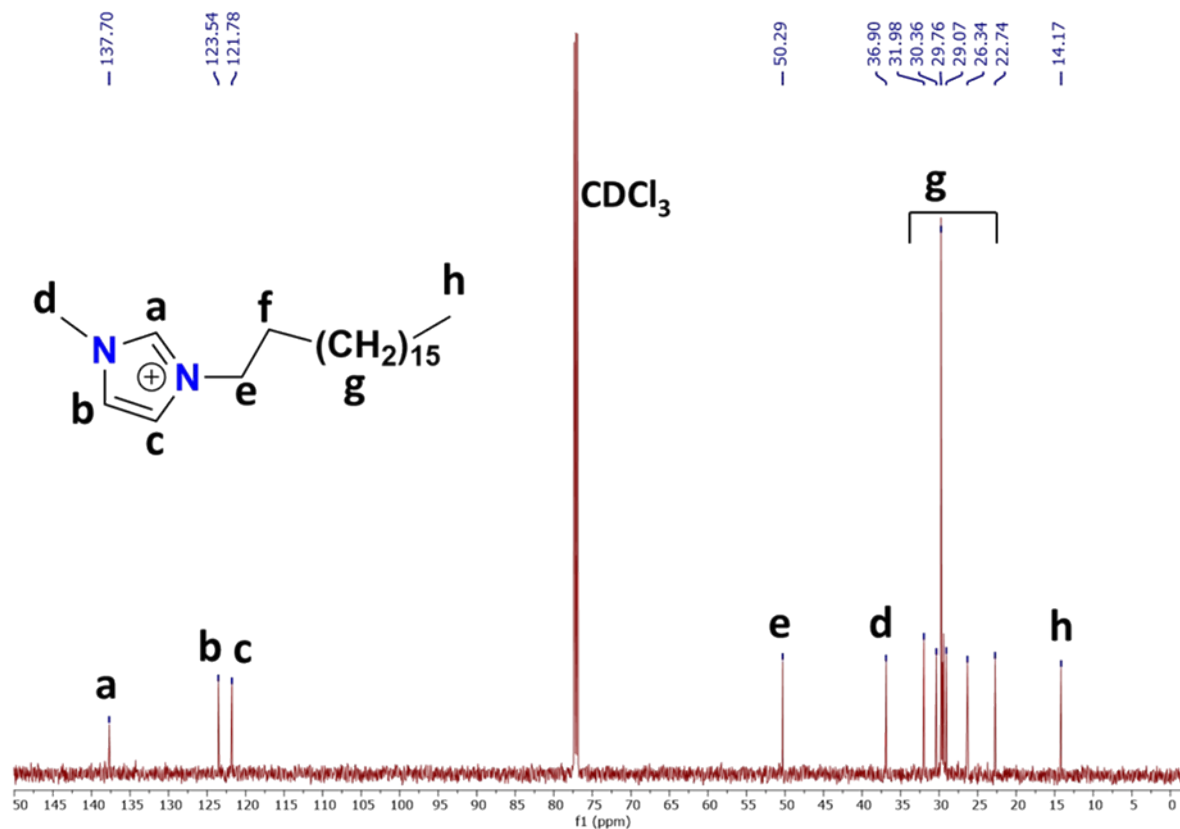


Fig. S2 ^{13}C NMR spectra of the synthesized ionic liquid.

Synthesis of wormlike fibrous mesoporous silica (WFNS)

For the biphasic synthesis of WFNS, initially, 3 g of 1-methyl-3-octadecyl-1H-imidazol-3-ium bromide ionic liquid (8.93 mmol) was dissolved in 150 mL of Mili Q water at 600 rpm for 30 minutes to form a micellar froth. Subsequently, 8 g (133.20 mmol) of urea, acting as the hydrolyzing agent, was added along with 5 mL of trimethylamine (35.87 mmol). Next, 8 mL (36.09 mmol) of TEOS dissolved in 50 mL of 1-decanol were slowly added to the above mixture over 30 minutes. The reaction mixture was then aged for 2 h with a slow stirring rate of 100 rpm. Afterwards, 5 ml of butanol was added and the reaction mixture was refluxed for 12 h at 90 °C. The newly formed white precipitates were centrifuged at 8000 rpm for 5 minutes washed three times with water and methanol and then dried in an oven at 70 °C overnight. For template removal, the white precipitates were refluxed twice with 0.2 N HCl-water (100 mL),

centrifuged, washed, and then dried in the oven overnight at 70 °C giving out 6.12 g of the pure product as WFNS.

Synthesis of CD incorporated silica material (CD@WFNS)

To produce the CD incorporated material, carbon dot precursors including 1.2 g of urea (19.9 mmol), 3 mL of formaldehyde (81.41 mmol), 1 g of sodium citrate (3.87 mmol), and 1.2 g of phytic acid (1.81 mmol) were loaded onto the above porous WFNS material (4 grams) and subjected to hydrothermal heating at 180 °C for 12 h. The resulting mixture was then centrifuged, thoroughly washed three times with water and methanol, and finally dried in an oven overnight at 60 °C, resulting in the material CD@WFNS.

Synthesis of CD@WFNS@Cl material

The standard synthetic procedure was employed for the covalent attachment of 3-CPTES to generate the CD@WFNS@Cl material. Specifically, 3 g of the previously synthesized CD@WFNS material was refluxed with 8 mL of 3-CPTES (34.18 mmol) in toluene at 110 °C for 24 h. After the reaction times, the mixture was allowed to cool and collected through centrifugation at 8000 rpm for 3 min. The product was then washed properly with toluene and methanol (3 times) and dried in an oven at 60 °C overnight to give 3.21 g of the product as CD@WFNS@Cl.

Synthesis of the final material CD@WFNS@DAB-AO

The final product was synthesized initially by refluxing 3 g of the CD@WFNS@Cl material with 2 g of DAB moiety (15.02 mmol) in acetonitrile at 80 °C for 12 h. After the reaction course, the material was isolated by centrifugation, washed with acetonitrile, and dried in the oven at 55 °C for 4 hours. The above isolated material was further used for amidoximation and was refluxed in ethanol at 85 °C for 12 hours with 2 g of hydroxylamine hydrochloride,

$\text{NH}_2\text{OH}\cdot\text{HCl}$, (28.78 mmol). Following the reaction, the mixture was cooled to room temperature, centrifuged at 8000 rpm for 2 minutes, washed thoroughly with ethanol and chloroform three times, and finally dried in an oven at 60 °C for 5 h, resulting in 3.39 g of the final material designated as CD@WFNS@DAB-AO. This obtained final material underwent comprehensive characterization using various analytical techniques and was evaluated for uranium detection and capture applications.

Photo-physical studies

The Photophysical investigations were conducted by preparing an aqueous dispersion of the material at a concentration of 15 mg per 50 mL. Before each spectral measurement, the suspension was vigorously mixed. Selectivity studies were performed with the chloride and nitrate salts of the following cations: Li^+ , Na^+ , K^+ , Cs^+ , Ca^{2+} , Mg^{2+} , Sc^{3+} , Sr^{2+} , Cr^{3+} , Mn^{2+} , Fe^{3+} , Co^{2+} , Ni^{2+} , Al^{3+} , Cu^{2+} , Pb^{2+} , Zn^{2+} , Cd^{2+} , Hg^{2+} , Ba^{2+} , Ce^{3+} , La^{3+} , Nd^{3+} , Gd^{3+} , VO^{2+} , and with the potassium salts of a wide range of anions, for example, SO_4^{2-} , CO_3^{2-} , NO_3^- , HSO_3^- , SO_3^{2-} , PO_4^{3-} in HEPES buffer. The spectra of UV-Vis were recorded within the 200–800 nm range. The fluorescence analyses were done within 520-800 nm, upon an excitation wavelength of 500 nm. The limit of detection (LOD) and that of quantification (LOQ) are calculated by methods of 3σ and 10σ through progressive addition of minute quantities described by titration experiments of specific uranyl ions respectively. The formula for LOD can be defined as 3σ , where $\sigma = \text{S.D} / \text{S}$, S.D is the standard deviation of 5 blank readings without the addition of analyte (uranyl ions) and S is the slope of the linear plot of fluorescence intensity vs concentration obtained during small incremental addition of the uranyl ions.

Adsorption Studies:

Batch adsorption experiments were carried out to examine the adsorption behavior of the material toward uranyl ions at the concentration range of 20-200 ppm for uranyl ions. In all, 5 mg of the material was mixed with 50 mL of the above-said analyte and shaken for 3 hours to

achieve saturated equilibrium in the dark and broad daylight separately. After the treatment, samples were filtered in a 0.45 μm micron filter and analyzed by ICP-MS. The parameters determined in the study variously were equilibrium adsorption capacity, plots of Langmuir and Freundlich, and kinetic parameters. The equilibrium adsorption capacity (Q_e) was derived from the formula $Q_e = (C_i - C_f) V / W$, where C_i and C_f are the initial and final concentrations of uranyl ions, V is the volume of the analyte, and W is the weight of adsorbent. Adsorption isotherms plots for Langmuir and Freundlich were evaluated and can be expressed by $C_e / q_e = C_e / q_{\text{max}} + 1 / q_{\text{max}} \times K_L$, where: C_e is the uranyl ions' equilibrium concentration, mg L^{-1} , q_e is the equilibrium adsorption capacity, mg g^{-1} ; q_{max} is the uranyl ions adsorption capacity on the adsorbent mg g^{-1} , and K_L is Langmuir adsorption constant. The Freundlich isotherm on the other hand can similarly be expressed as $\ln q_e = \ln K_f + 1 / n \ln C_e$ where q_e and C_e are the equilibrium adsorption capacity, mg g^{-1} and the equilibrium concentration of the uranyl ions and n the Freundlich constant respectively. The graft yield was calculated based on the weight change using the following equation; Graft yield (%) = $W_2 - W_1 \times 100 / W_1$, where W_1 & W_2 are the initial (before grafting: CD@WFNS@Cl) and final total weight (after grafting: CD@WFNS@DAB-AO) of the material.

Similarly, pH dependent experiments were carried out in both light and dark at varying pH values from 3 to 9, as above, with material derivations of 10 mg in 40 ppm, 500 ml uranium-spiked simulated seawater, followed by centrifugation at 8000 rpm for 15 minutes and syringe filtration using a 0.45 μm micron filter, and submitted to ICP-MS for final concentration analysis. Rate kinetic studies were performed at various concentrations of 4, 10, 20 ppm uranium-spiked seawater by taking 10 mg of material in 500 mL of the respective analyte concentration. Following the promising results, kinetic studies were conducted in both light and dark conditions for 25 ppm (500 mL) uranium-spiked seawater. To conduct interference and selectivity studies, 10 mg of the material was incubated in diluted seawater conditions (500

mL, 2 ppm, 5 ppm mixed cations spiked seawater) for ~3 h. The pseudo-first-order equation

$$\ln(q_e - q_t) = \ln q_e - (k_1)t$$
 and pseudo-second-order kinetics equation
$$\frac{t}{q_t} = \frac{1}{k_2 q_e^2} + \frac{t}{q_e}$$
 were utilized for analysis kinetics rate order. In the above equations, q_e and q_t are the number of uranyl ions adsorbed per unit mass of adsorbent at equilibrium and time t , respectively, and k_1 (min^{-1}) and k_2 ($\text{g}^{-1} \text{ mg min}^{-1}$) are the pseudo-first-order and pseudo-second-order rate constants, respectively.

Bio sensing Studies

Biosensing investigations involved the use of *Artemia* nauplii, chosen for their cost-effectiveness and suitability as a biosensing animal model. *Artemia salina* cysts were hatched under aerobic conditions to obtain the larvae, specifically *Artemia* nauplii, for in vivo imaging studies. Approximately ~25 *Artemia* nauplii were placed in 20 mL of a brine solution and treated with 80 μL of the probe material suspension (10 mg / 25 mL) for 3 hours. After incubation, the organisms were transferred onto glass slides and observed using bright and fluorescent filters on an OLYMPUS BX53 microscope. Subsequently, solutions containing uranyl salt at concentrations of 60 μL of 10^{-5} M were introduced, and images were captured using the microscope. Safety protocols were strictly followed during the handling of uranium salts.

Anti-microbial studies

The antimicrobial performance and activity of the final material (CD@WFNS@DAB-AO) against various bacterial strains, namely *Bacillus subtilis*, *Escherichia coli*, and *Pseudomonas aeruginosa*, was monitored in the dark and in light. First, overnight cultivation of the above bacterial colonies was conducted separately at 37°C in nutrient broth in light and darkness.

Plates were prepared by dispensing 20 μ L of the material suspension into a nutrient agar. 100 μ L of inoculated broth was spread to agar plates containing material suspension. The plates were incubated at 37°C in dark and light conditions separately. Testing the viability of bacterial was performed using the dilution plate method. The inhibition rate was then calculated according to $IR = (Ci - Cf) / Ci \times 100$, where Ci is the number of initial bacterial colonies (untreated with the material) and Cf refers to that of the final bacterial colonies, which were treated with the material suspension.

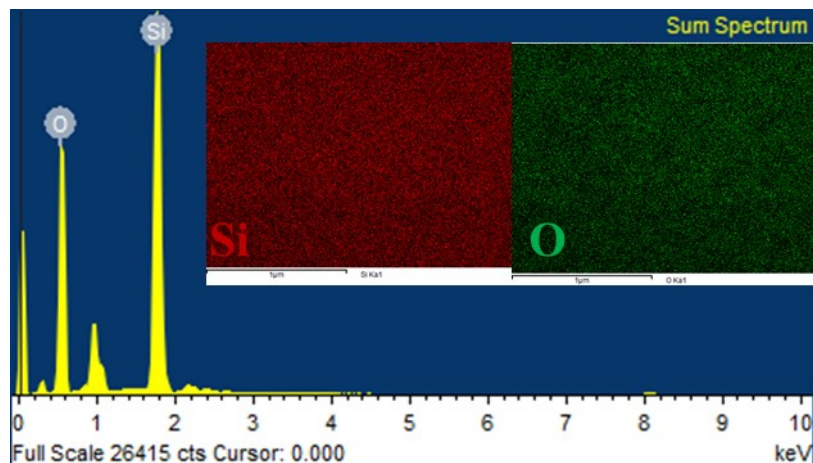


Fig. S3 The EDX spectrum and elemental mapping (inset) of worm like fibrous mesoporous silica (WFNS) showing signals of silicon and oxygen elements.

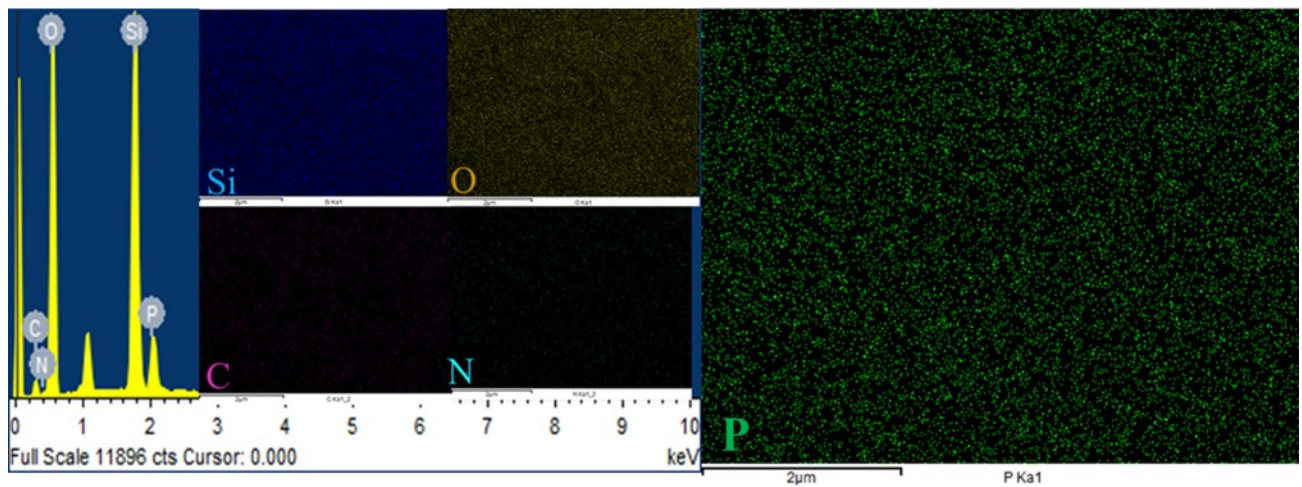


Fig. S4 The EDX spectrum and elemental mapping of the carbon dot embedded WFNS material (CD@WFNS) showing successful N, P doped carbon dot incorporation.

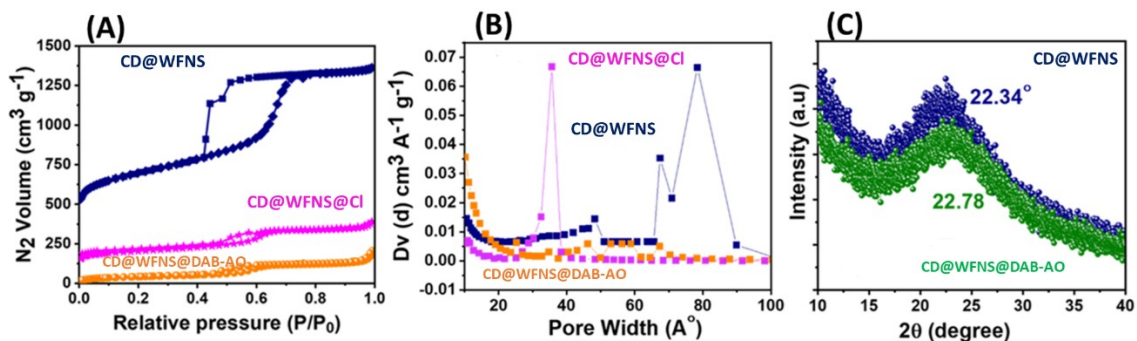


Fig. S5 (A) The BET surface area & pore size distribution of the materials. (B) The high-angle PXRD showing the amorphous nature of the materials.

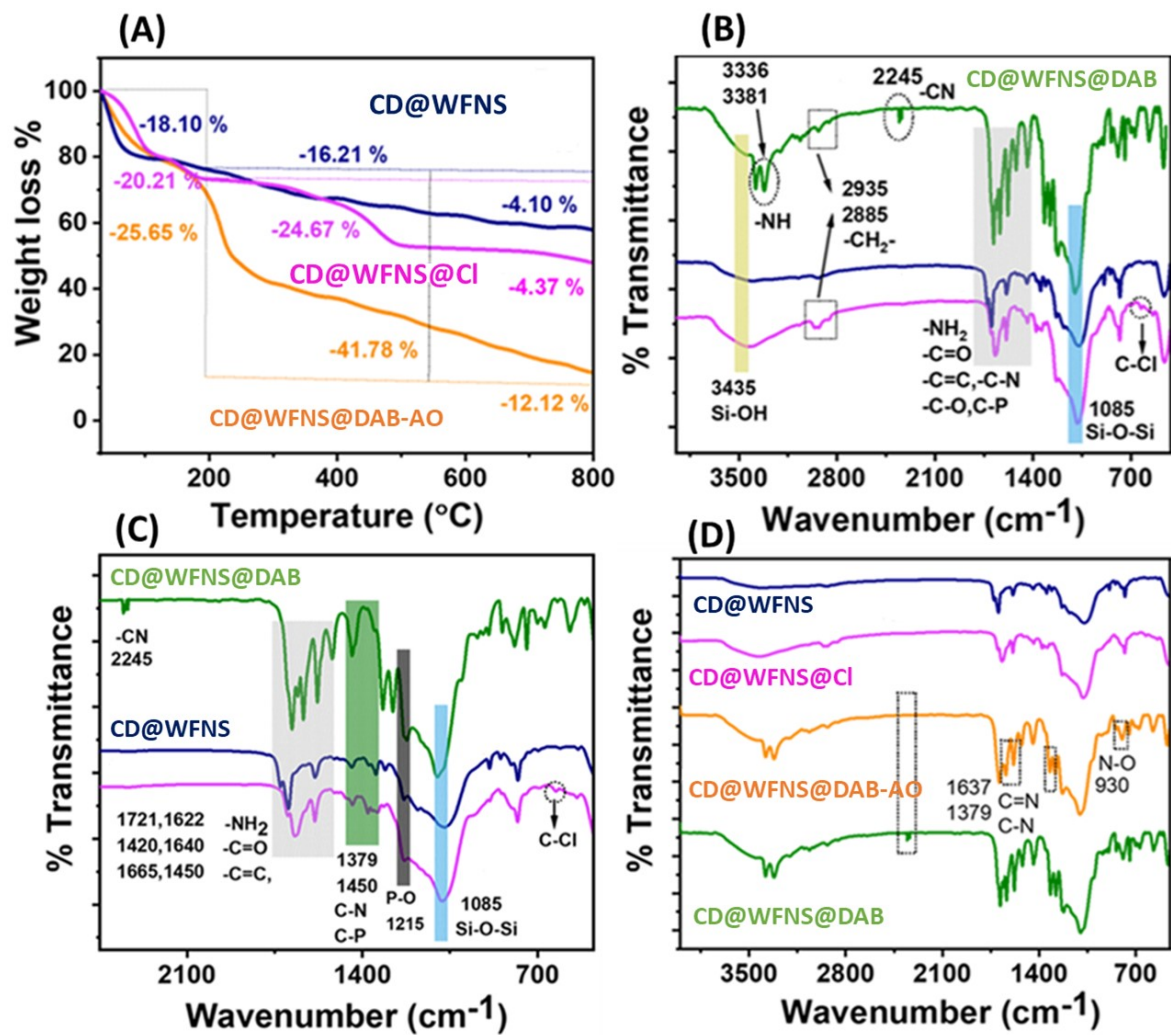


Fig. S6 (A) TGA profiles of the synthesized materials. (B-D) The comparison of the FTIR spectra of the synthesized materials CD@WFNS, CD@WFNS@Cl & CD@WFNS@DAB-AO.

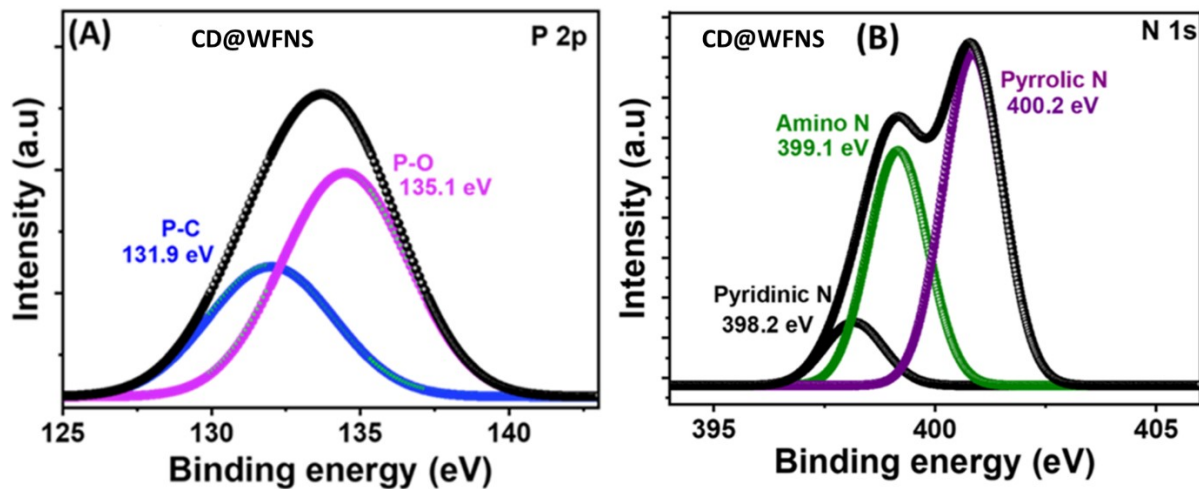


Fig. S7 (A, B) The P-2p & N 1s core shell spectra of the CD@WFNS material.

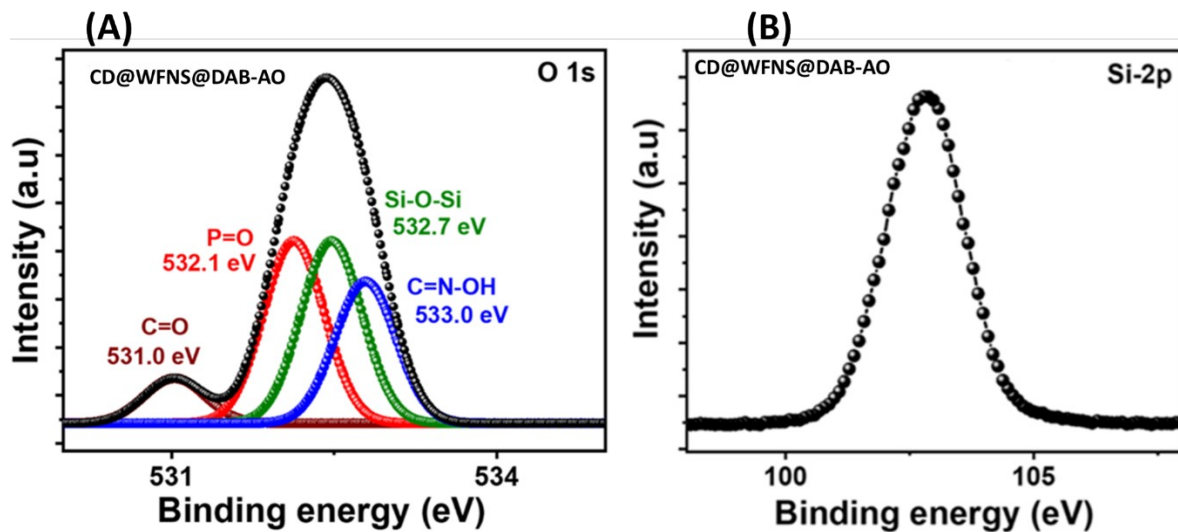


Fig. S8 (A, B) The O 1s & Si-2p core shell spectra of the final material CD@WFNS@DAB-AO.

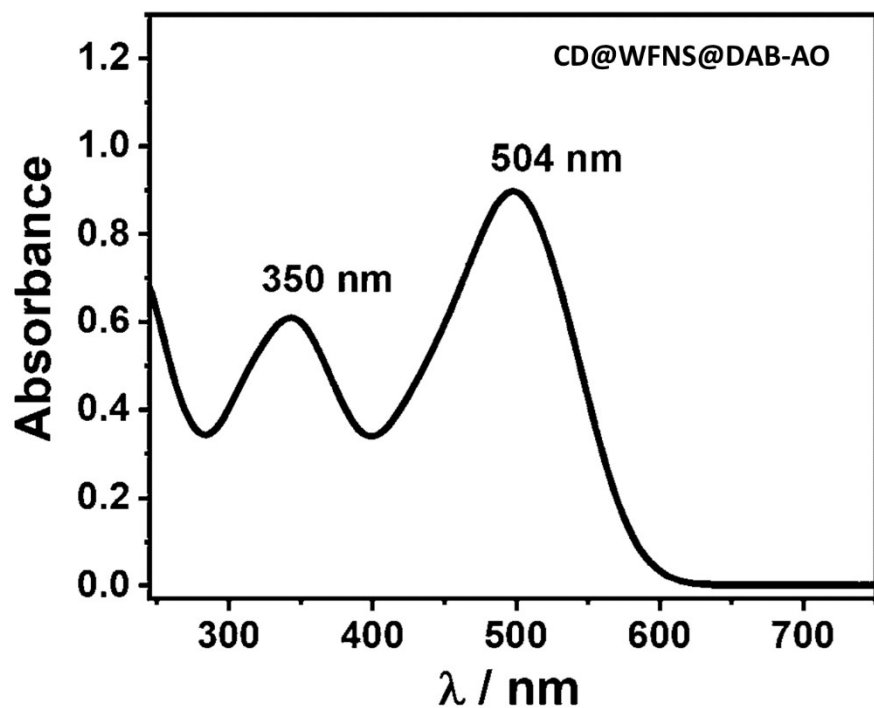


Fig. S9 The UV-Vis spectra of the final material CD@WFNS@DAB-AO.

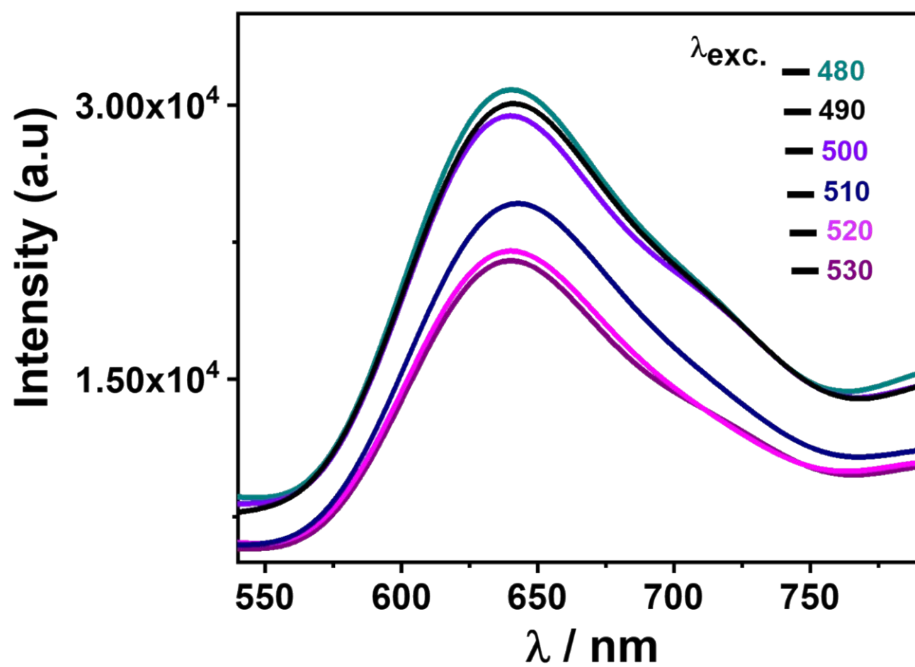


Fig. S10 The excitation-independent behaviour of the final material showing consistent emission spectra.

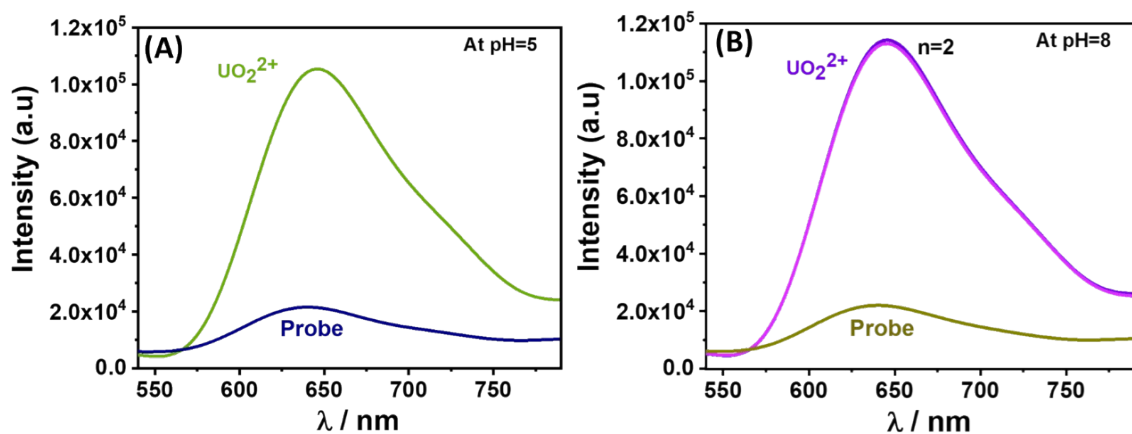


Fig. S11 (A-B) The pH-dependent selectivity studies of the probe material.

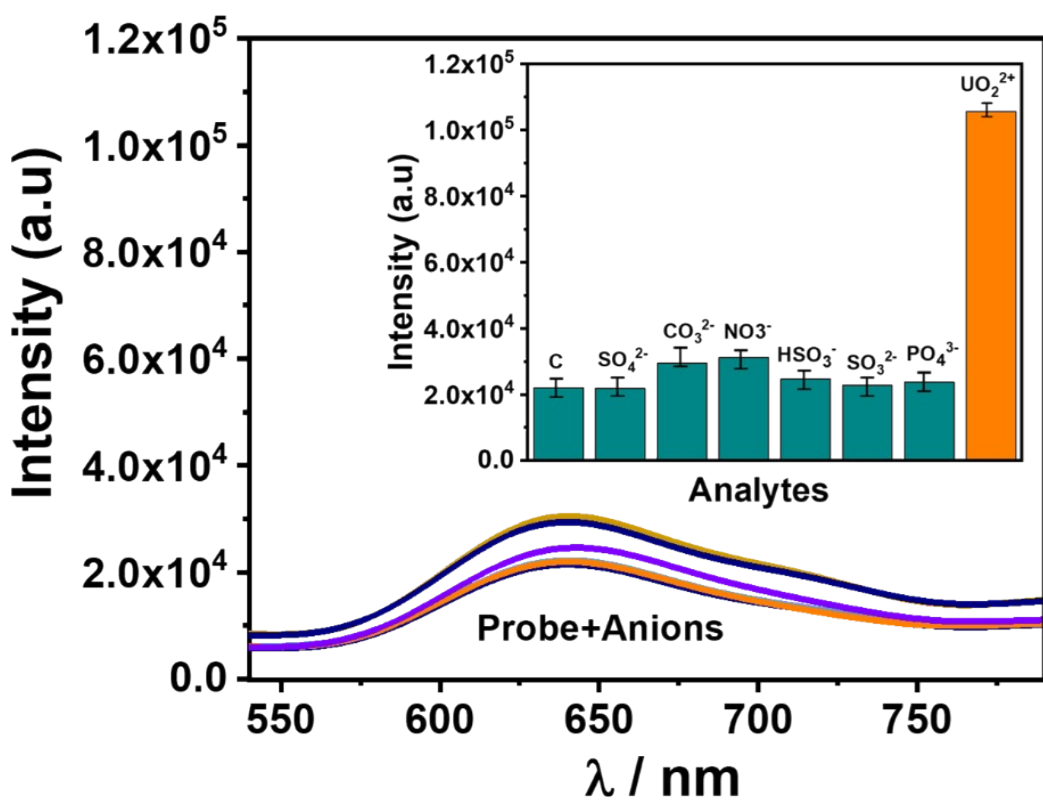


Fig. S12 The selectivity studies of the probe material with the anions (inset: the relative emission intensity).

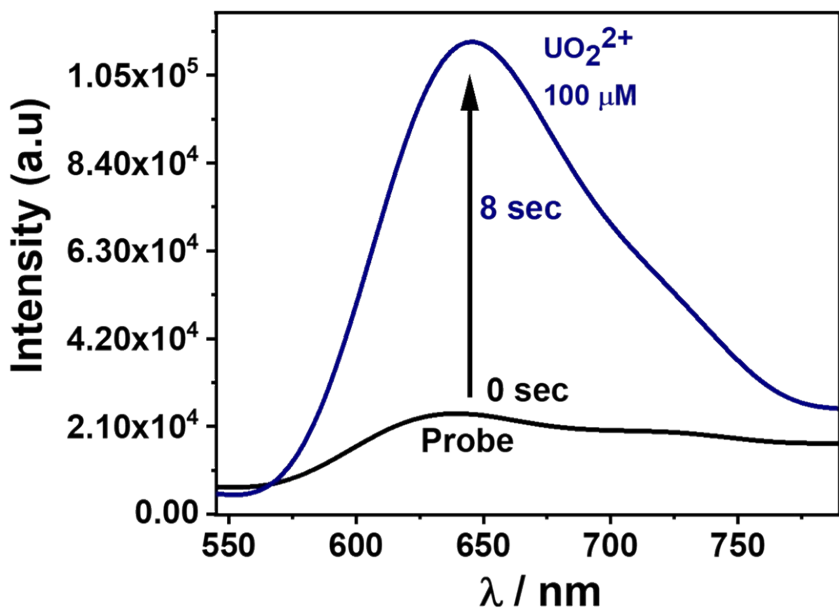


Fig. S13 The quick fluorescence response of the probe material towards uranyl ions.

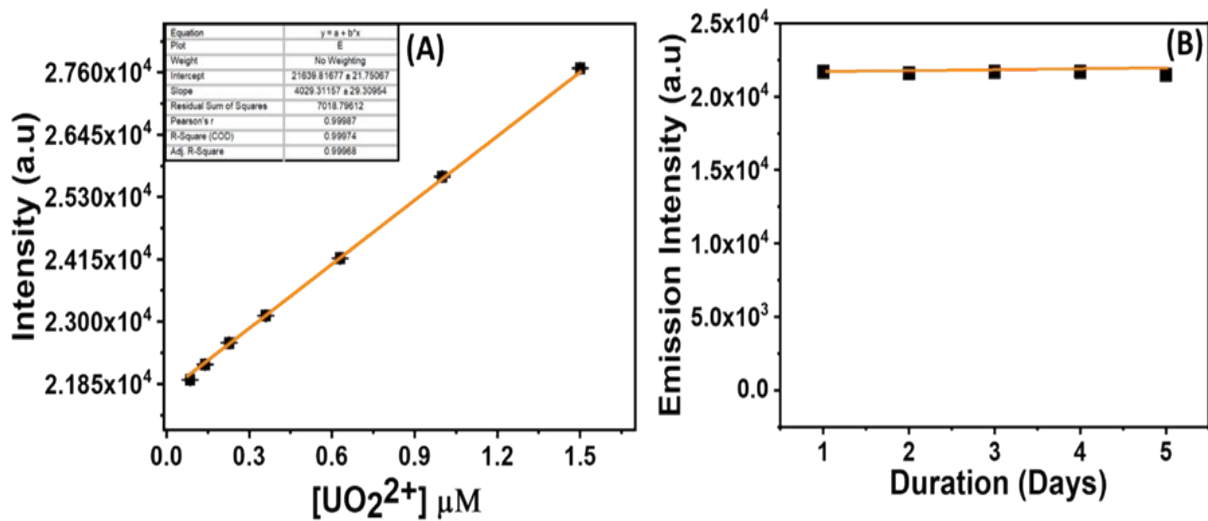


Fig. S14 (A-B) The linear range fitting and fluorescence emission stability plot.

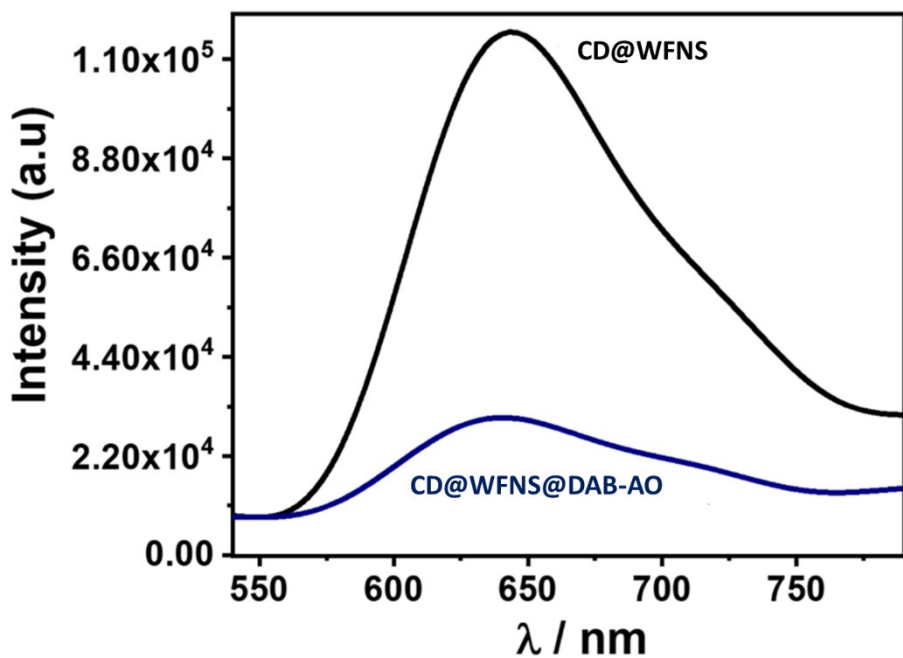


Fig. S15 The comparison of the fluorescence emission plot of the material CD@WFNS and final material CD@WFNS@DAB-AO

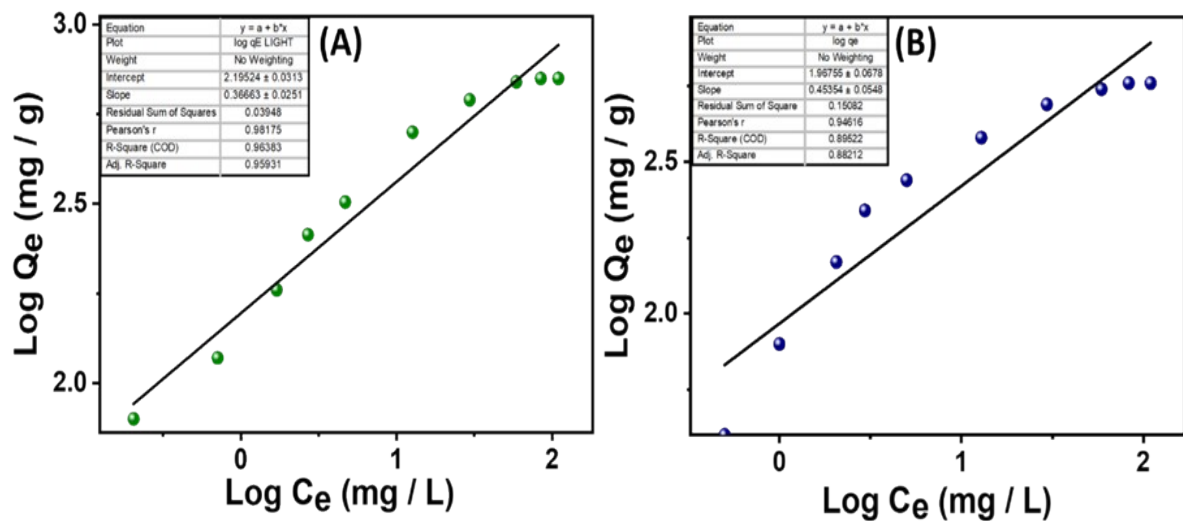


Fig. S16 (A, B) The Freundlich adsorption isotherm of the material under light and dark conditions.

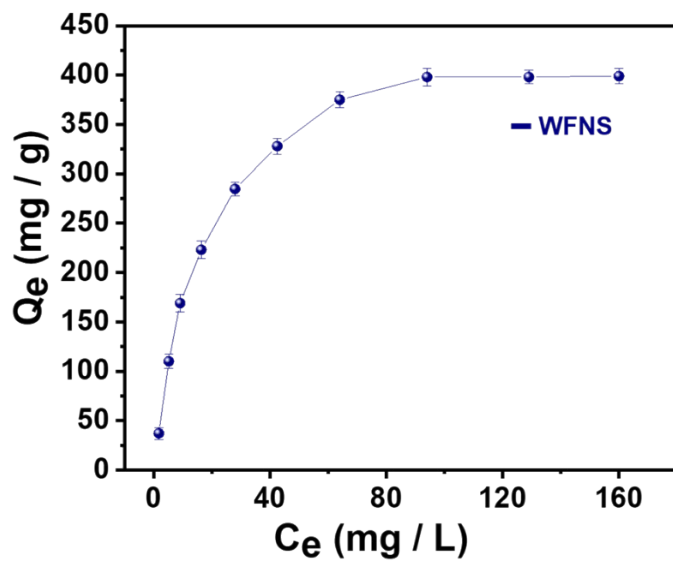


Fig. S17 The equilibrium adsorption capacity (q_e) of the bare WFNS towards uranium.

Table S1 The Competitive extraction performance table

Analyte	C_i (in ppm)	C_f (in ppm)	E (%)
Li	19.23	18.45	Negligible
Na	20.12	19.23	Negligible
K	20.42	19.56	Negligible
Ca	18.25	17.89	Negligible
Mg	20.67	19.23	Negligible
Sr	19.13	18.20	Negligible
V	19.34	17.45	Negligible
U	20.12	0.34	98.31 %
Cr	20.01	18.27	Negligible
Mn	19.13	19.01	Negligible
Fe	20.12	18.12	Negligible
Co	19.32	19.04	Negligible
Ni	20.34	20.01	Negligible
Cu	20.12	19.89	Negligible
Zn	20.01	19.90	Negligible
Hg	19.89	19.84	Negligible
Cd	19.45	19.02	Negligible

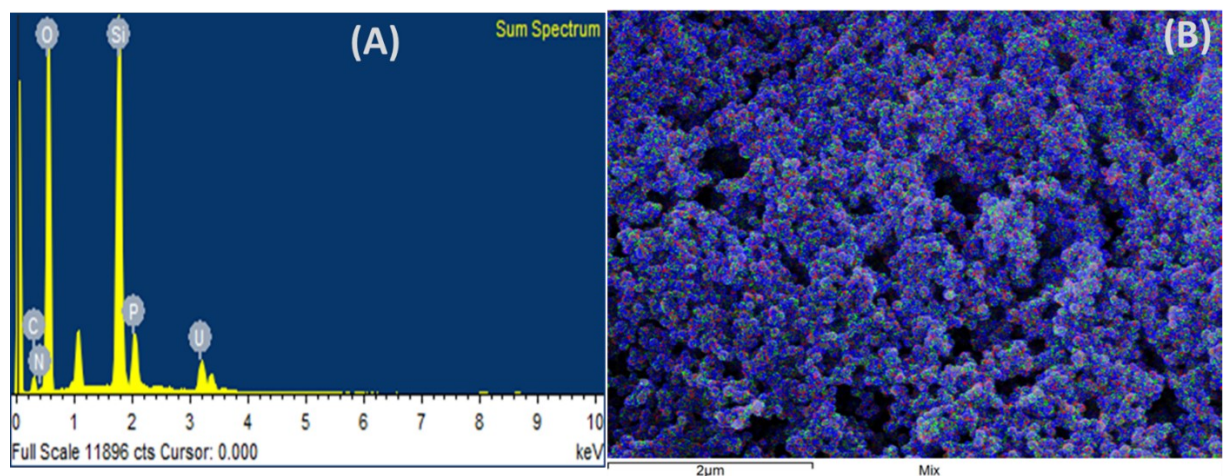


Fig. S18 (A-B) The EDX spectrum & elemental colour mapping (mix) of the material showing uranium adsorption.

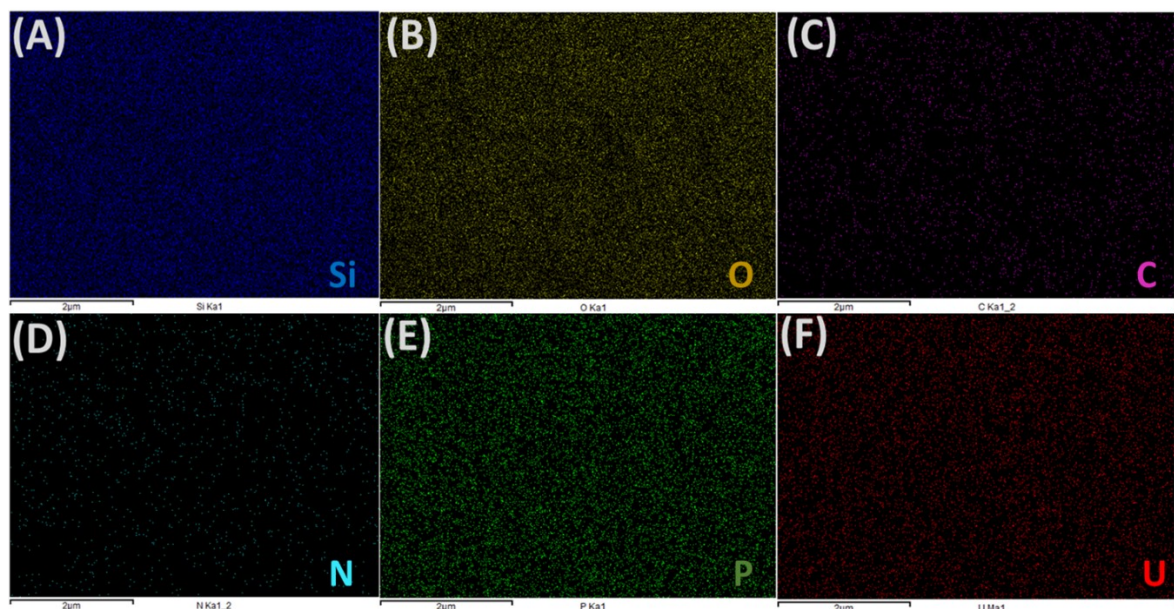


Fig. S19 (A-F) The EDX elemental colour mapping of the material after the uranium adsorption.

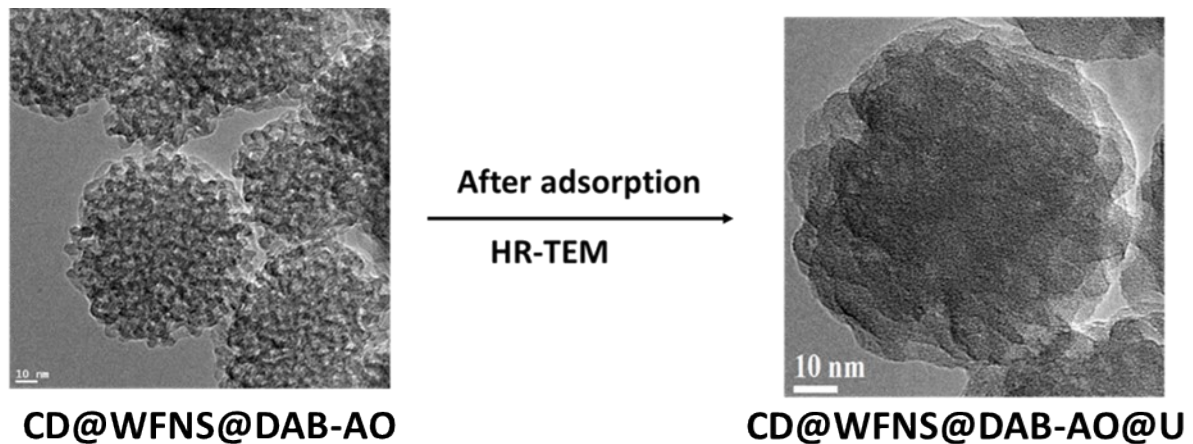


Fig. S20 The HR-TEM analysis of the final material before and after uranium adsorption.

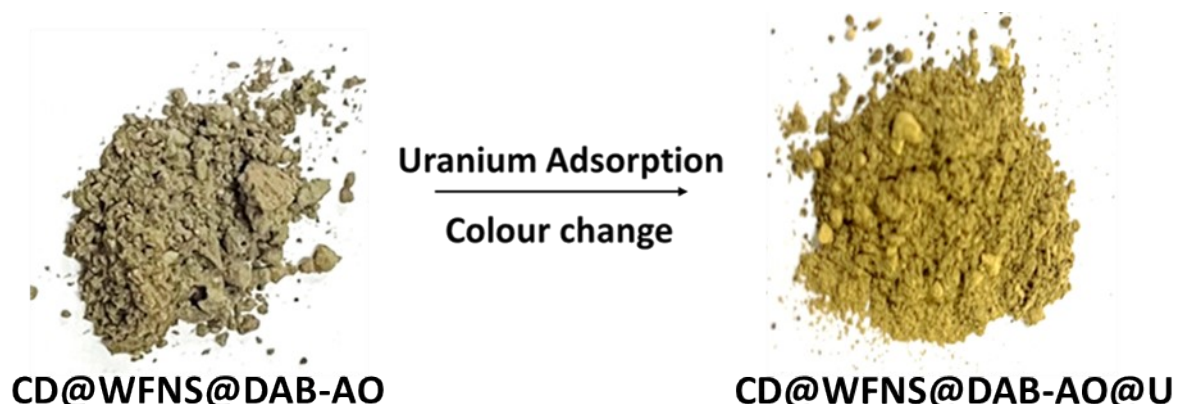


Fig. S21 The colour change picture of the material before and after the uranium adsorption (aqueous studies).

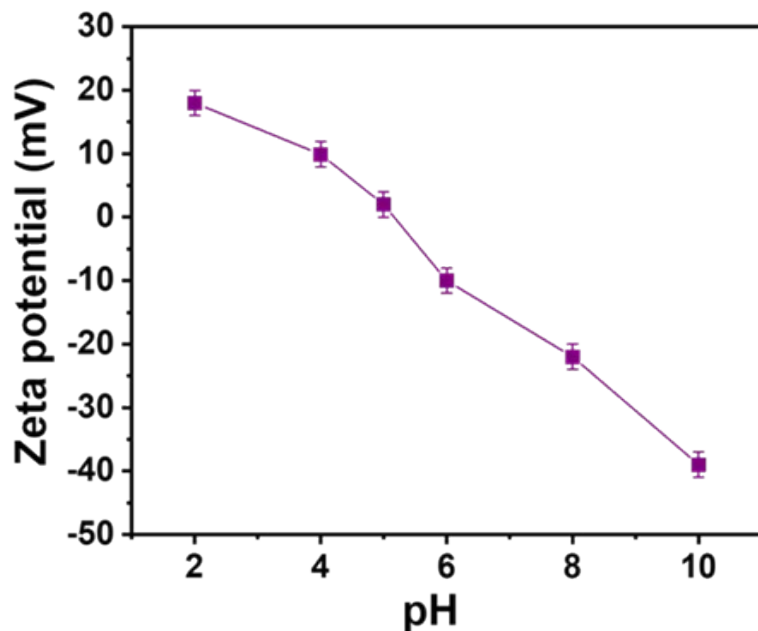


Fig. S22 The zeta potential measurements of the final material at various pH values.

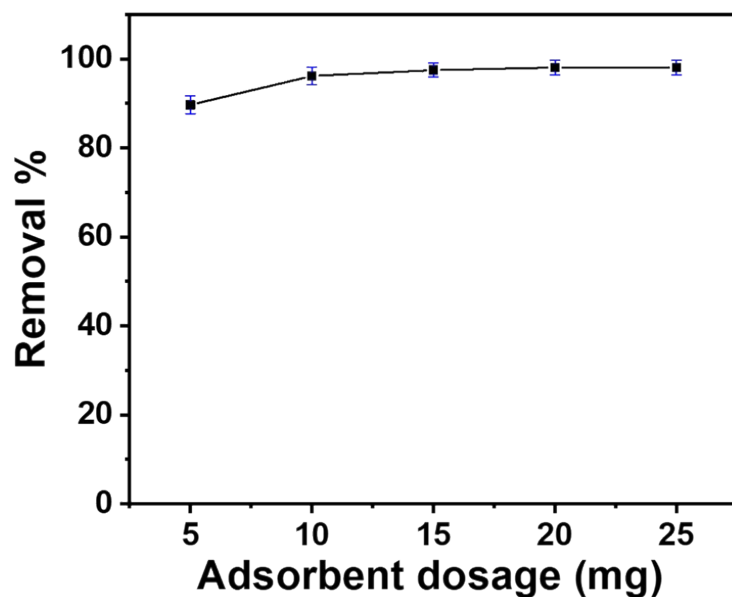


Fig. S23 The removal efficiency (% R) plot as a function of varying dosage of the material.

Table S2 The adsorption kinetic parameters

Analyte (U) Spiked seawater concentration (S.S.W)	q_e (Experimental)	k_2	q_e (calculated)	R^2
4 ppm	199	0.99	201.61	0.99
10 ppm	345	1.01	384.61	0.99
20 ppm	398	1.124	420.12	0.99
25 (Light)	570	1.10	613	0.99
25 (Dark)	445	1.08	478.46	0.98

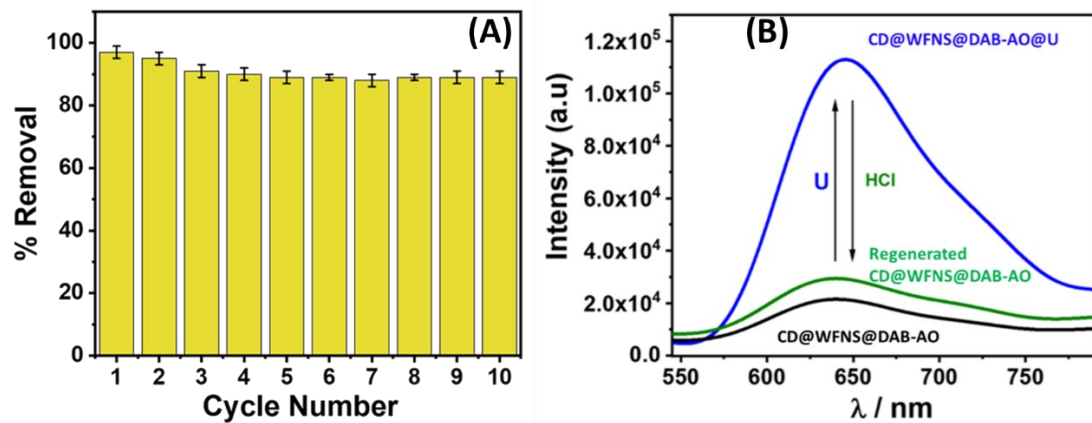


Fig. S24 (A) The uranium removal percentage by the material over 10 cycles. (B) The fluorescence tracking during the regeneration of the material.

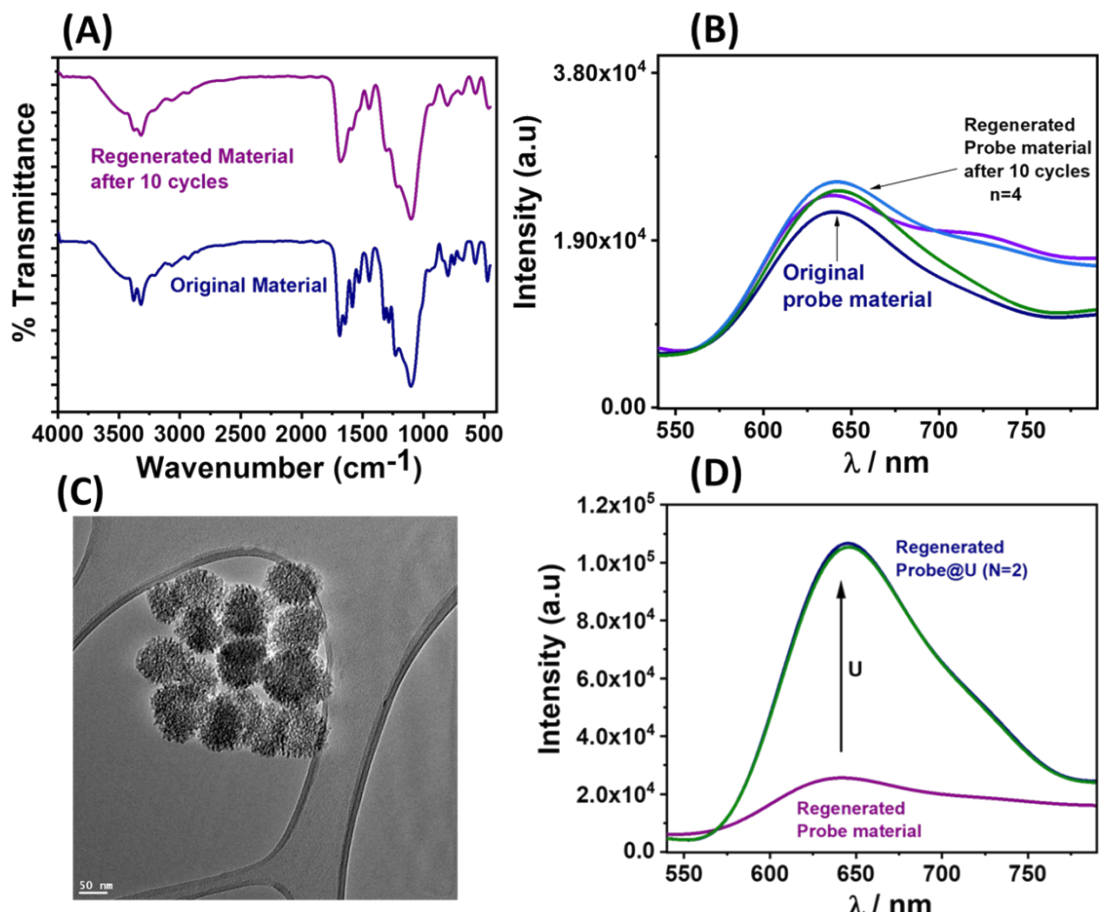


Fig. S25 (A-D) The characterization plots of the regenerated material after 10th cycle by FT-IR, Fluorescence response and TEM showing intact functionality, optical behaviour, and structural integrity.

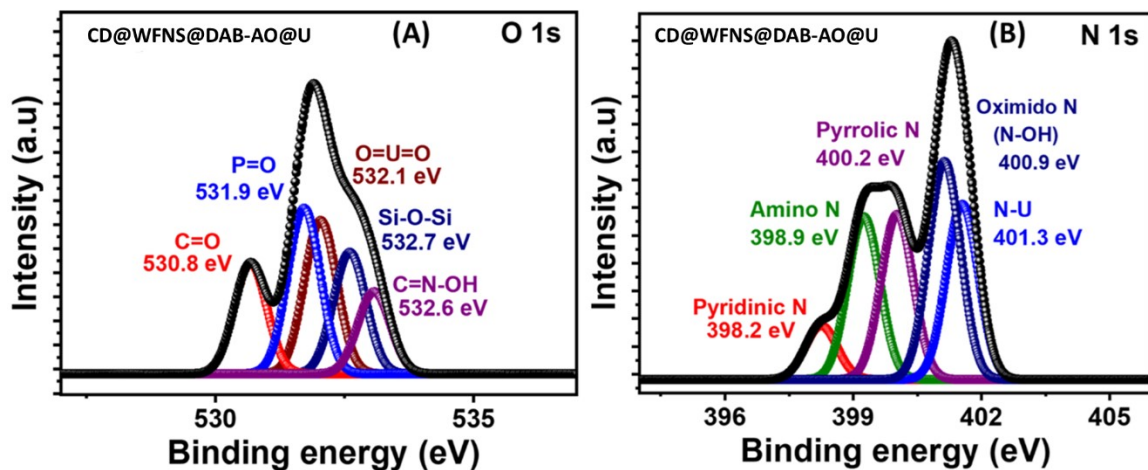


Fig. S26 (A, B) The core shell O 1s & N 1s spectra of the uranium adsorbed material.

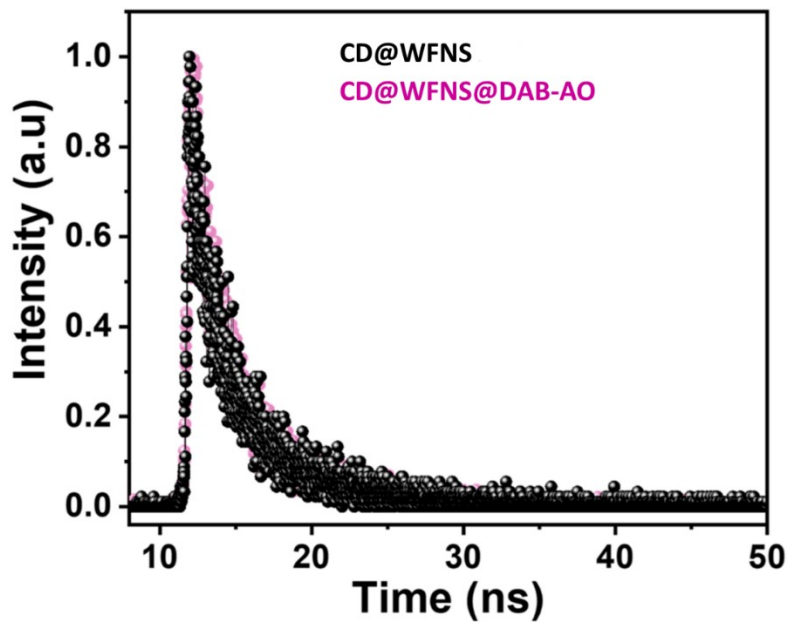


Fig. S27 The Fluorescence lifetime spectra of the materials (CD@WFNS = 2.60 ns, $\chi^2 = 1.01$; CD@WFNS@DAB-AO = 2.71 ns, $\chi^2 = 1.1$)

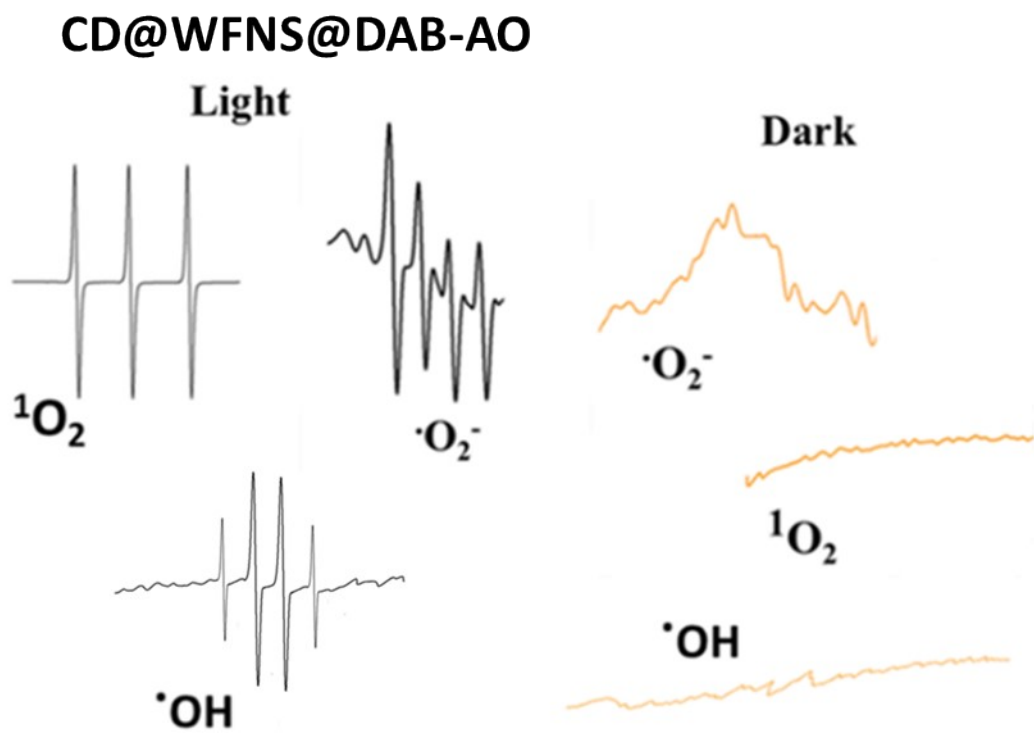


Fig. S28 The EPR spectra of ROS trapped using DMPO and TEMPO in light & dark conditions.

Field Test (Natural seawater uranium extraction)

For uranium extraction from seawater, the field study was conducted at our established experimental salt farm (ESF) where gallons of natural seawater are collected for salt manufacturing. Our field study involved 3 sets, where typically in a set, 5 mg of the adsorbent material was filled in the dialysis bag and subject to under seawater deployment. After a certain interval of time, the bags were taken out and washed properly with the distilled water to remove the excess salt contamination that may be present at the bag's surface by stirring the recovered bags in 100 ml of distilled water at 500 rpm for 30 minutes. Afterward, the material was recovered from the bags using HPLC water (10 ml) centrifuged (10000 rpm) and simultaneously washed 3 times to remove any residual ions. Finally, the material obtained was stripped using 1 N HCl (20 mL) and stirred for 15 min at 200 rpm, followed by centrifugation, syringe filtration (0.45 μ m filter), and subject to ICP-MS analysis.

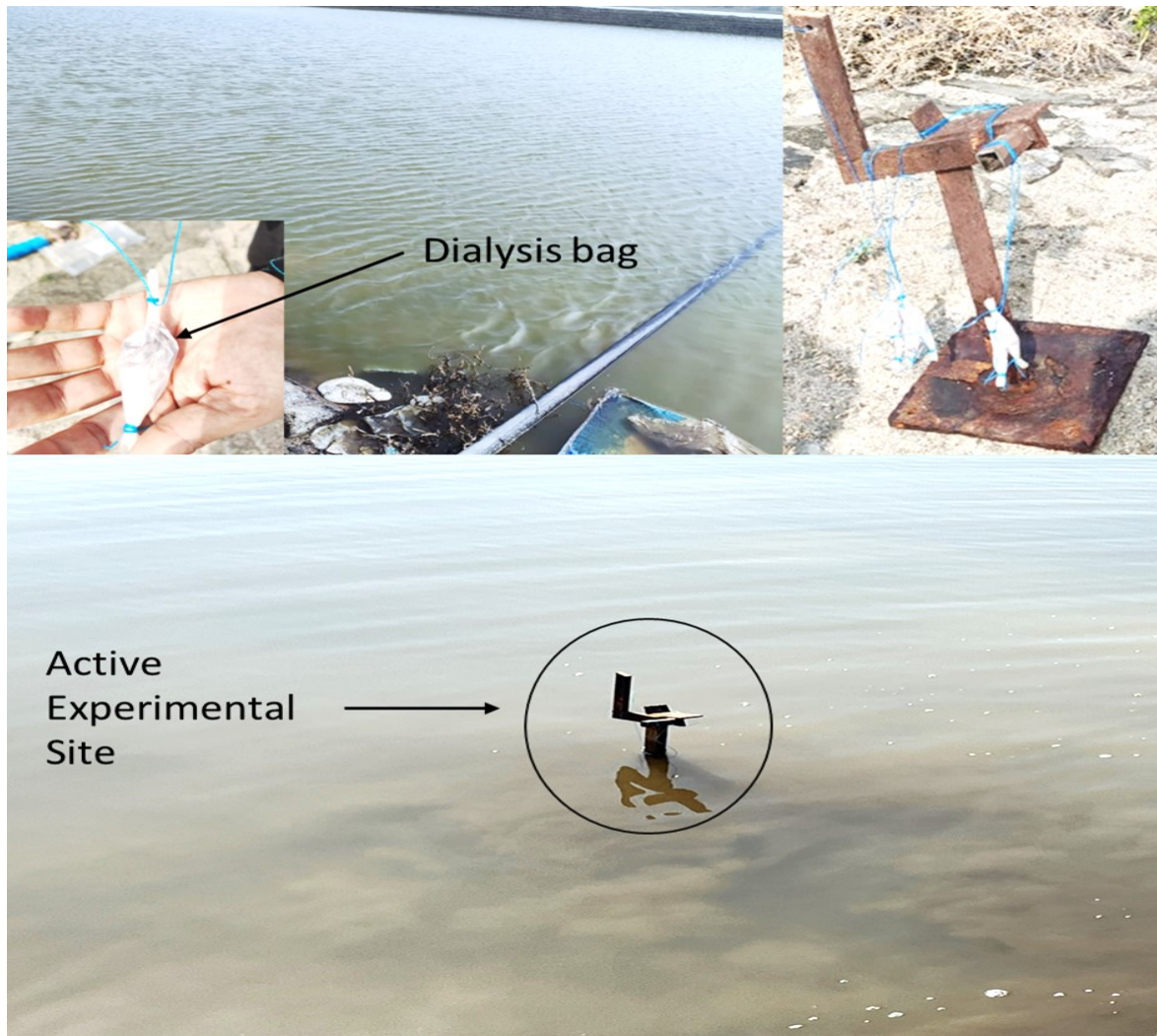


Fig. S29 Field test experiments for Uranium adsorption from seawater at Experimental Salt Farm (ESF) of CSIR-CSMCRI.

Table S3. The performance comparison table of different materials towards uranium.

Material	Detection (LOD) & Response	Adsorption capacity(A.C)/ (Seawater (S.W))	Dual Functions (Detection + Adsorption)	Photocatalytic Reduction	Biofouling Property	Biosensing	Ref
Materials for fluorescence detection of Uranium							
Luminescent Mesoporous Metal–Organic Framework (MOF)	0.9 $\mu\text{g/L}$ Turn Off	×	×	×	×	×	11
Carbon Dots (AIE)	6.53 ppb Turn Off	×	×	×	×	×	13
N-CDs	20 nM Turn Off	×	×	×	×	×	14
Coordination Polymer	1.42 μM Turn Off	×	×	×	×	×	15
UiO-66-NH ₂ MOF	19.04 ppb Turn Off	×	×	×	×	×	16
Anionic Co-MOFs	0.13 μM Turn Off	×	×	×	×	×	17
Zn-MOF	2.92 ppb to 0.86 ppb Turn Off	×	×	×	×	×	18
Eu-MOF	2.7 nM Turn Off	×	×	×	×	×	19
Olefin-linked COF	21.25 nM Turn Off	×	×	×	×	×	20
UiO-66-NH ₂ MOF	15.3 nM Turn On	×	×	×	×	×	21
Eu-COF	1.36 nM Turn On	×	×	×	×	×	22
Materials for adsorption of Uranium							
Porous aromatic framework	×	A.C: 82.5 mg / g, (Seawater (S.W): 5.79 mg/g 56 days)	×	×	×	×	26
A 3D hierarchical porous amidoxime fiber	×	(S.W: 11.50 mg/g 90 days)	×	×	×	×	27
Poly(amidoxime) architecture	×	(S.W: 17.57 mg/g, 30 days)	×	×	×	×	28
Amidoxime-functionalized halloysite nanotubes	×	A.C: 456.24 mg g ⁻¹ (S.W: 9.01	×	×	×	×	30

		mg/g, 30 days)						
Ion-imprinting MOF	×	A.C: 461 mg g ⁻¹ (S.W:7.35 mg/g)	×	×	×	×	×	31
Ionic MOF	×	A.C: 1489.13 mg g ⁻¹ , (S.W: 28.2 mg/g, 25 days)	×	×	×	×	×	32
Anionic MOF	×	A.C:1336.8 mg g ⁻¹ (S.W: 9.42 mg/g, 30 days)	×	×	×	×	×	33
2D uranium-organic framework	×	A.C:1.0 g/g, (S.W: 0.64 mg/g/day)	×	×	×	×	×	34
Covalent polymer aerogels	×	A.C: 203.01 mg g ⁻¹ (S.W:10.43 mg/g in 28 days)	×	×	×	×	×	35
Amidoximated Metal–Organic Framework	×	A.C: 426.3 mg g ⁻¹ No Seawater ×	×	×	×	×	×	36
Polyamidoxime-functional β-cyclodextrin adsorbents	×	A.C: 944.75 mg g ⁻¹ , (S.W:10.9 mg/g/day)	×	×	×	×	×	37
Imidazole-based COF	×	A.C: 902 mg g ⁻¹ (S.W: 6.9 mg/g/day)	×	✓	×	×	×	38
Triazine-linked 2D COF	×	A.C:10.9 g/g, (S.W:34.5 mg/g 42 days)	×	✓	×	×	×	39
Cyano-functionalized graphitic carbon nitride	×	A.C: 2644.3 mg g ⁻¹ (S.W: 0.26 mg/g/7 days)	×	✓	×	×	×	40
Composite fiber	×	A.C: 990.60 mg g ⁻¹ (S.W:11.76 mg/g, 56 days)	×	✓	×	×	×	41
Polymeric peptide	×	A.C:139.47mg g ⁻¹ (S.W:7.12 mg/g)	×	×	✓	✓	×	43
Zwitterion Hydrogels	×	A.C:196.12 mg g ⁻¹ , (S.W: 6.1 mg g ⁻¹ 30 days)	×	✓	✓	✓	×	44

Amidoxime Group-Anchored Single Cobalt Atoms	×	A.C: 687 mg g ⁻¹ (S.W:9.7 mg g ⁻¹)	×	×	✓	×	45
Materials for Detection & Adsorption of Uranium							
sp ² carbon-conjugated fluorescent covalent organic framework (COF)	6.7 nM Turn Off	A.C:427 mg g ⁻¹ No Seawater (S.W)	✓	×	×	×	6
Photonic Crystal Hydrogel	10 × 10 ⁻⁹ M	A.C: 169.67 mmol kg ⁻¹ No Seawater (S.W)	✓	×	×	×	7
Conjugated microporous polymers (CMPAO)	1.7 × 10 ⁻⁹ M Turn Off	A.C: 251.9 mg g ⁻¹ No Seawater (S.W)	✓	×	×	×	8
3-D COF	4.08 nM Turn Off	A.C: 955.3 mg g ⁻¹ No Seawater (S.W)	✓	×	×	×	9
Luminescent Terbium–Organic Framework	1.07 and 0.75 ppb Turn Off	A.C: 83.43 mg/g No Seawater	✓	×	×	×	12
Zn-MOF	1.2 × 10 ⁻⁸ M Turn Off	A.C: 632 mg/g No Seawater (S.W)	✓	×	×	×	49
MOF hydrogel composite	1.2 ppt Turn Off	A.C: 549.0 mg/g No Seawater (S.W)	✓	×	×	×	50
Sp ² COF	8.3 nM Turn Off	A.C: 436 mg g ⁻¹ No Seawater (S.W)	✓	×	×	×	51
Co (II)-MOF	0.13 μM Turn Off	A.C: 129.8 mg g ⁻¹ No Seawater (S.W)	✓	×	×	×	52
N-carbon dot-hydrogel composite	8.4 nM Turn Off	A.C: 194 mg g ⁻¹ No Seawater (S.W)	✓	×	×	×	54
Lanthanide-organic framework material (IHEP-24)	0.1–3 mM (LR)	A.C: 193.5 mg g ⁻¹ No Seawater (S.W)	✓	✓	×	×	63
Functionalized P,N doped-CD@Wormlike	7.4 nM Turn On	710 mg g ⁻¹ (S.W:12.13 mg/g/30 days)	✓	✓	✓	✓	This Work

Fibrous Silica (CD@WFNS@DAB- AO)							
---	--	--	--	--	--	--	--